

Article

Gait Pattern Identification Using Gait Features

Min-Jung Kim, Ji-Hun Han, Woo-Chul Shin  and Youn-Sik Hong *

Department of Computer Science and Engineering, Incheon National University, Incheon 22012, Republic of Korea; alsjwds47@inu.ac.kr (M.-J.K.); jin4884@inu.ac.kr (J.-H.H.); crepas2@inu.ac.kr (W.-C.S.)

* Correspondence: yshong@inu.ac.kr

Abstract: Gait analysis plays important roles in various applications such as exercise therapy, biometrics, and robot control. It can also be used to prevent and improve movement disorders and monitor health conditions. We implemented a wearable module equipped with an MPU-9250 IMU sensor, and Bluetooth modules were implemented on an Arduino Uno R3 board for gait analysis. Gait cycles were identified based on roll values measured by the accelerometer embedded in the IMU sensor. By superimposing the gait cycles that occurred during the walking period, they could be analyzed using statistical methods. We found that the subjects could be identified using the gait feature points extracted through the statistical modeling process. To validate the feasibility of feature-based gait pattern identification, we constructed various machine learning models and compared the accuracy of their gait pattern identification. Based on this, we also investigated whether there was a significant difference between the gait patterns of people who used cell phones while walking and those who did not.

Keywords: IMU (Inertial Measurement Unit); gait analysis; healthcare; internet of things; gait pattern recognition



Citation: Kim, M.-J.; Han, J.-H.; Shin, W.-C.; Hong, Y.-S. Gait Pattern Identification Using Gait Features. *Electronics* **2024**, *13*, 1956. <https://doi.org/10.3390/electronics13101956>

Academic Editors: Ilaria Sergi and Teodoro Montanaro

Received: 19 April 2024

Revised: 12 May 2024

Accepted: 14 May 2024

Published: 16 May 2024



Copyright: © 2024 by the authors. Licensee MDPI, Basel, Switzerland. This article is an open access article distributed under the terms and conditions of the Creative Commons Attribution (CC BY) license (<https://creativecommons.org/licenses/by/4.0/>).

1. Introduction

Walking is the most common health activity in daily life and the first activity to be affected by physical disabilities. Gait analysis is the systematic study of human walking using detailed observations and measurements of bodily movements, mechanics, and muscle activity. The purpose of gait analysis is to identify any abnormalities in the way a person walks, evaluate walking efficiency, and assess the overall biomechanical health of the individual. Gait analysis can help improve pedestrian safety and security in public spaces, transportation systems, commercial facilities, and more. Motion detection technology such as CCTV can be used to identify dangerous situations, and pedestrian identification can be used in secure systems to prevent unauthorized access. Gait analysis also has applications in business, such as providing customized products and services by identifying customer preferences and behaviors through their movements. Currently, it is being commercialized in the healthcare sector, such as using treadmills to detect gait and provide exercise therapy.

Identifying walking patterns has important applications in many aspects of health, security, and business. Some studies have suggested a link between walking and brain health, highlighting that walking can support brain function and improve cognition [1]. Other studies are investigating the interaction between walking and cognition in patients with geriatric diseases such as Alzheimer's [2–4]. These studies are expected to help us understand the impact of walking patterns on cognition and brain health and to aid in the early detection and management of these conditions. They also show the potential for innovative uses of walking pattern identification in health and medicine, providing useful information to monitor and treat patient conditions [5].

Recent research related to gait analysis includes the use of multiple infrared cameras [6–8] and markers [9] to analyze the movement of markers in an indoor area and the use of foot pressure sensors [10] and treadmills to analyze plantar pressure distribution [11]. The

infrared camera method has limitations in terms of location, the inconvenience of wearing the equipment, and cost, while the pressure sensor method requires the equipment to be customized to the size of a person's foot. Treadmills are less useful for the elderly and patients who have difficulty walking.

Lin, C.-L. et al. [12] implemented deep learning neural network models using pedestrian color image sequences as an input and found them to be effective for pedestrian detection and recognition. They extracted moving silhouette figures from the walking image sequences and used the correlation between the original and new silhouettes as a primitive feature of human walking.

Lee et al.'s work [13] describes a sensor compensation algorithm that transforms an unstable sensor coordinate system into a stable anatomical coordinate system and enhances the distinction between individual gait patterns through the introduction of 2D cyclogram features.

Recently, many effective research methods using inertial sensors have been proposed. T. Gujarathi et al. [14] compared joint angles measured using an inertial sensor and a 3D motion capture system and presented results indicating that the deviation was not significant. H. Kim et al. [15] showed that the joint movement patterns of the hip and knee joints during walking can be recognized using an MPU-9150 IMU (Inertial Measurement Unit). Methods using inertial sensors offer the convenience of wearing equipment, have no space restrictions, and can be implemented at a low cost. IMUs with built-in inertial sensors are small, easy to attach to the body, and relatively inexpensive (USD 150 to USD 200). Furthermore, IMU sensor-based gait analysis does not require additional equipment to be installed to configure the experimental environment.

An IMU consists of a gyroscope, an accelerometer, and a geomagnetic sensor. An accelerometer is a sensor that measures the acceleration of an object, while a gyroscope measures the rotational speed and angular velocity (rad/s) of an object. A magnetometer is a sensor that detects the magnetic field of an object. In the previous studies using IMUs, about 70% of the experiments were conducted by attaching them to the shanks or ankles of the subjects [16–21]. These studies mainly focused on extracting gait parameters such as gait speed, gait cycle, cadence, stance time, and swing time.

In this study, a wearable module with an IMU [14,15,22] was used for gait analysis on flat ground. Unlike treadmill walking, people walk at different speeds and move their feet at different angles on flat ground. A person's gait parameters are variable depending on their physical condition, gender, and age. By superimposing gait cycles over a period of walking, it may be possible to extract significant gait parameters using statistical methods. If statistically significant discrete gait features can be extracted from continuous gait data, it will be possible to identify gait patterns using these gait features.

Our proposed method to eliminate the uncertainty brought by highly variable gait data involves superimposing gait cycles. The advantage of superimposing gait cycles is that it can eliminate outliers and identify statistically significant features.

The three feature points extracted in our proposed method varied depending on the collected data. However, the superimposed gait cycles were not expected to have large statistical deviations, and we confirmed through experiments that the gait cycles converged to a constant value after preprocessing. This means that the gait cycles stabilized as walking continued. This was also the purpose behind our attempt at superimposing gait cycles.

This paper is organized as follows. Section 2 describes a wearable module with an embedded IMU sensor and a method of gait cycle recognition used in this study. Section 3 discusses the relationship between left and right foot walking. Section 4 proposes a method of gait pattern identification using gait features. Section 5 applies the proposed method to a real application model. Section 6 concludes this work.

2. Gait Cycle Recognition Using IMU Sensors

On a flat surface, a person's gait pattern (walking speed, steps per minute, etc.) is not constant, but they repeat a regular gait cycle. The gait cycle consists of eight gait phases

from Heel Strike to Terminal Swing. In this study, we built a wearable module using the MPU9250 IMU sensor (by InvenSense Inc., San Jose, CA, USA) for the experiment. Although the IMU sensor consisted of nine-axis sensors, the gait parameters (roll, pitch, and yaw) extracted from the three-axis acceleration sensor were mainly utilized for gait parameter analysis. For this paper, we focused on the roll value, which could track changes in leg movement. By repeatedly superimposing roll data with the periodicity in the gait cycle for a certain walking time, statistically significant gait parameters could be extracted. We extracted three statistically significant features from the superimposed graphs and used them for statistical modeling.

2.1. Gait Cycle

The gait cycle is divided into a stance phase and a swing phase, as shown in Figure 1 [23]. The stance phase, which accounts for 60% of the total gait, is when the sole of the foot is in contact with the ground and supports the body's weight. The swing phase, which accounts for the remaining 40% of the gait, is when the foot is in the air. The gait cycle can be further broken down into eight patterned gait phases. The stance phase can be divided into five phases, from Heel Strike (HS) to Pre-Swing (PS), and the swing phase can be divided into three phases, from Toe-Off (TO) to Terminal Swing (TS). The main characteristics of each part of the gait cycle are as follows:

- Heel Strike (HS): Gait begins in the Heel Strike phase, which is the moment when the heel touches the ground. At this point, the foot is placed on the ground and the leg movement begins.
- Loading Response: In this phase, weight is placed on the legs and the body is lifted upward. This process propels the pedestrian's body further forward.
- Mid-Stance: In this phase, the body weight is fully supported on one foot and the legs are straight. The body stabilizes in the Mid-Stance phase.
- Terminal Stance: In this phase, the legs are responsible for moving the body forward. The knees should be kept pinned and the weight should be shifted forward.
- Pre-Swing (PS): In this phase, the sole of the foot begins to push off the ground. This acts as a springboard for the next gait cycle.
- Toe-Off (TO): This is the moment when the sole of the foot leaves the ground, preparing for the next gait cycle.
- Mid-Swing (MS): The Mid-Swing phase is entered with the legs crossed in midair. This is when knee extension is maximized to prepare for the next phase, the Heel Strike.
- Terminal Swing (TS): In this phase, the gait cycle is completed as the legs prepare to return to the ground from the air.

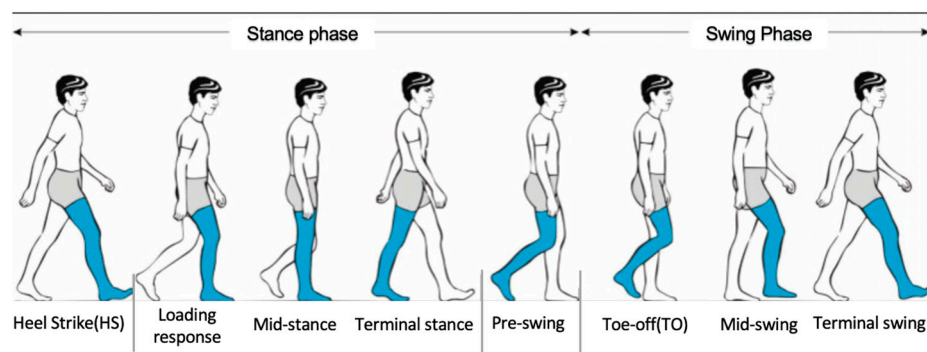


Figure 1. Gait phases and detailed gait steps in a gait cycle [23].

2.2. IMU Sensor

IMU sensors are used to simplify gait analysis without any restrictions on the configuration of the experimental environment. An IMU sensor basically consists of a three-axis gyroscope, a three-axis accelerometer, and a three-axis magnetic sensor. An accelerometer is a sensor that measures the acceleration of an object on the x -, y -, and z -axes. It is used to

measure the acceleration of an object or to detect shocks, tilt, etc. A gyroscope measures the rotational speed and angular velocity (rad/s) of an object along the x -, y -, and z -axes. The values measured by a gyroscope are used to calculate the pitch value. A magnetometer is a sensor that measures the azimuth angle and magnetic field of an object on the x -, y -, and z -axes. IMU sensors are categorized into six-axis and nine-axis sensors depending on whether they have a magnetometer, with six-axis IMU sensors being more common. It is also possible to use two IMU sensors instead of one.

The locations where IMU sensors are mounted on the body are mainly concentrated on the lower body, such as the top of the foot, the back of the foot, the thigh, and the shank. This representative study of gait analysis using IMU sensors attempted to distinguish the Heel Strike (HS) point and the Toe-Off (TO) point in the gait cycle by attaching six-axis IMU sensors (accelerometers and gyroscopes) to both shanks. Using the raw data acquired from the IMU sensors, the research objective was to distinguish the stance phase from the swing phase in the gait cycle.

The MPU 9250 IMU sensor is a nine-axis IMU sensor. It consists of three accelerometer axes, three gyroscope axes, three magnetometer axes, and one temperature axis. The coordinate system of a three-axis sensor is shown in Figure 2.

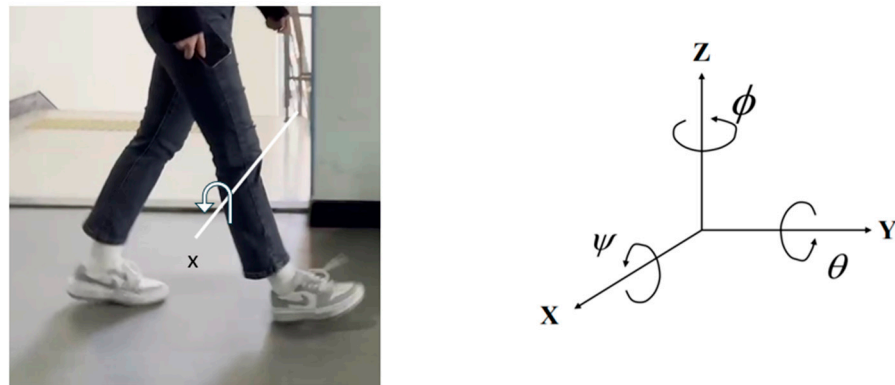


Figure 2. The x -axis (left) and MPU9250 coordinate system (right) when the module is attached to the right shank.

Roll, pitch, and yaw can be calculated from the raw data measured by the MPU-9250's built-in sensors. The radius of rotation indicated by roll, pitch, and yaw when the sensor is attached to the ankle is shown in Figure 2. The yaw value can be calculated from the raw data measured by the magnetic sensor. The rotation speeds in the x , y , and z axis directions are used to determine the rotation of an object. The pitch and yaw values are used to determine movement, such as the direction of rotation of the ankle during walking. However, since the object of analysis in this paper was straight walking on a flat surface, the pitch and yaw values were not processed.

The roll value is the angle of the knee, and it can be used to determine how much the knee extends and flexes. The roll value was obtained using data measured by the accelerometer. The acceleration of the accelerometer in the x , y , and z axis directions was related to the tilt of the object and could be calculated based on that. The roll value was found using Equation (1). Notice that A_x , A_y , and A_z represent the acceleration values of the x -axis, y -axis, and z -axis, respectively.

$$\psi = \text{atan} \left(\frac{A_y}{\sqrt{A_x^2 + A_z^2}} \right) \quad (1)$$

2.3. Configuration of a Wearable Module

Since an IMU sensor is worn on the body to collect data, we chose the MPU-9250 for its small size. The Arduino Uno R3 model was used as an embedded board for a wearable

module. Although the Arduino Nano model has an advantage in terms of size and ease of mounting on the body, we chose the Uno R3 model to utilize the HC-05 and HC-06 Bluetooth modules instead of the Nano's built-in Bluetooth module. The HC-05 and HC-06 modules are devices that transmit and receive data via Bluetooth wireless communication and are mainly used in embedded systems such as Arduino or Raspberry Pi boards. By adding ankle pads to the embedded board, we built a wearable module that could be attached to the body.

The wearable module implemented for use in gait experiments is shown in Figure 3. The MPU-9250 was mounted on the Uno R3 board and connected to the HC-05. The board was bonded to the ankle pads. HC-05 operated in master mode, whereas HC-06 operated in slave mode. The raw data measured by the MPU-9250 sensor were received by the HC-05, which transmitted them to the HC-06. The HC-06 transmitted the data to the server via Bluetooth.



Figure 3. Data transmission process using the wearable module.

2.4. Roll Data-Based Gait Cycle Recognition

The raw data measured by the accelerometer were converted into analyzable roll data through preprocessing and data refinement such as outlier removal and filtering. Figure 4a shows the preprocessing of raw data with a Kalman filter, and Figure 4b shows the results after removing outliers. Figure 4b shows a graph of gait cycles that were extracted and continuously superimposed, with the red lines being the outlier gait cycles.

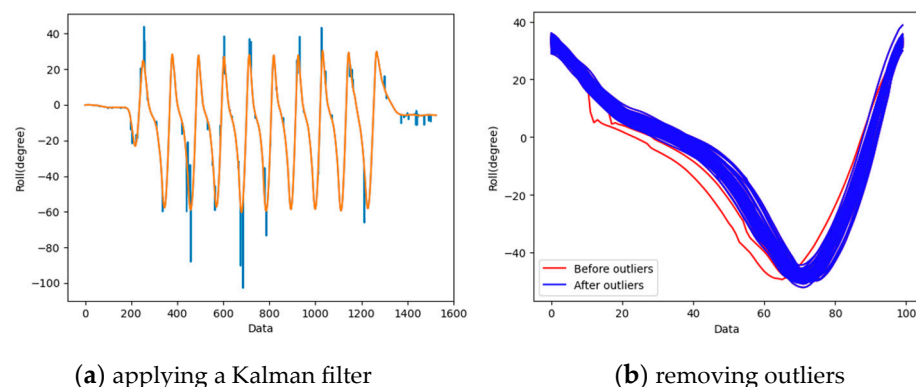


Figure 4. Preprocessing applied to raw data.

The beginning stage of the gait cycle, “Foot-Flat”, is the state when the foot is flat on the ground while the person is standing. However, this cannot be used as a starting point because each subject has a different Foot-Flat state point. In order to classify the gait cycle with certainty, we identified the gait cycle as the Toe-Off (TS) point (marked with a blue dot), corresponding to the minimum roll value, and the Heel Strike (HS) point

(marked with a red dot), corresponding to the maximum roll value, as shown on the left side of Figure 5. The TS point and HS point correspond to the beginning and end of the gait cycle, respectively. The gait cycle can be identified based on these two points, and thus gait parameters can be extracted based on the gait cycle.

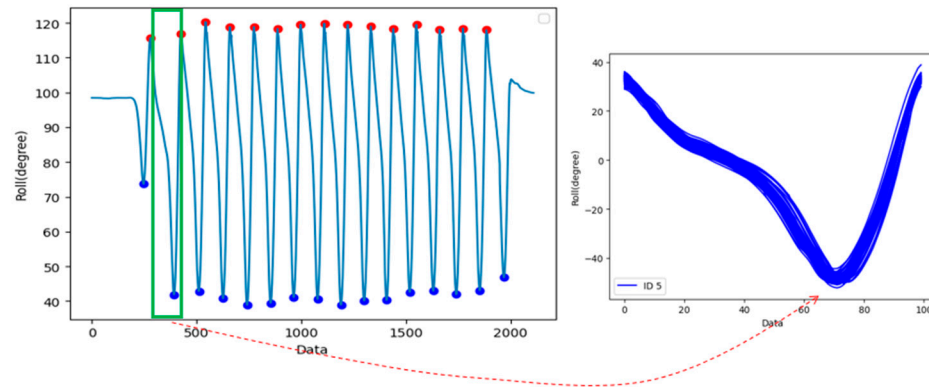


Figure 5. (left) TS points (marked with blue dots) and HS points (marked with red dots) and (right) the superimposed gait cycles for the subject (ID 5).

We split the roll data into sub-graphs for each gait cycle and then overlaid each sub-graph by aligning it with the beginning of the gait cycle. The right side of Figure 5 shows the superimposed graph for subject 5. The graph generated by overlaying gait cycles describes the gait characteristics of subject 5. By overlaying gait cycles, we can identify the statistical characteristics of the gait cycles.

2.5. Experimental Conditions and Subject Information

The subjects' natural walking was measured in a 15-meter-long flat area. To induce normal walking, the subjects went through two practice walks before starting the gait measurement. Fourteen volunteers (six men and eight women) with no physical disabilities participated in this experiment. The average age of the participants was 24 years (23 to 29 years), and the average height was 167 cm (156 cm to 190 cm). They were fully informed of the purpose and procedures of this experiment and gave their consent to participate in it.

3. Relationship between Left and Right Foot Walking Based on Gait Parameters

Although the left and right feet perform similar functions in walking, their use, efficiency, and roles in movement can vary due to a wide range of factors. In a healthy and typical gait, there is an expectation of symmetry between the left and right feet in terms of timing, force distribution, and range of motion. Symmetry is often an indicator of efficiency and normal gait patterns. The fundamental biomechanical processes that govern walking apply to both feet, which go through similar gait phases, such as the stance and swing phases, regardless of being the left or right foot.

Although perfect symmetry is rare, a functionally symmetric gait is often the goal of rehabilitation. Small differences are normal, but significant asymmetries may indicate underlying issues. Through biomechanical and kinematic analysis, we can quantitatively evaluate the similarities and differences between left and right foot walking. For this, gait parameters such as stride length, cadence, and the stance/swing time ratio are compared. In this study, we analyzed the differences between left and right foot walking using TO and HS.

The subjects wore the wearable modules attached to the knee protector pads on both shanks. The first step was to start with the left foot. Each subject was asked to walk a total of 10 times. As shown in Table 1, the average values of the gait time (unit: 1/100 s) of the right foot stabilized as the experiment was repeated. Therefore, the number of footsteps

after preprocessing also converged to a certain value. However, the standard deviation (SD) of the gait time of the right foot was larger than that of the left foot.

Table 1. Comparison of left and right foot gait characteristics after preprocessing.

Trial	Left Foot			Right Foot		
	Mean (1/100 s)	SD (1/100 s)	Gait Numbers	Mean (1/100 s)	SD (1/100 s)	Gait Numbers
1st	54.39	8.71	23	51.35	17.37	20
2nd	54.91	11.46	23	56.94	19.95	26
3rd	53.96	9.73	23	54.68	20.86	22
4th	54.48	16.13	23	54.09	16.77	22
5th	53.77	13.95	22	54.23	22.05	22
6th	54.39	17.29	23	60.94	14.27	16
7th	51.91	18.22	23	53.86	24.11	22
8th	54.57	21.04	23	53.54	14.78	24
9th	52.83	11.16	23	52.75	16.53	20
10th	54.35	19.58	23	53.04	15.57	23
Avg.	53.96	14.73	22.9	54.54	18.23	21.7

As shown in Table 1, the gait numbers of the left and right feet did not match, which caused a discrepancy in the gait cycles of the left and right feet. Thus, a direct comparison of the gait cycles based on the gait number was not feasible due to the lack of matching gait cycles between the two feet. Without overlapping gait numbers, we could not directly compare the same gait events across the left and right feet. Therefore, we performed separate analyses for each foot regarding HS and TO to understand the gait characteristics of each foot.

The visualizations shown in Figure 6 provide insights into the distributions of the HS and TO values and the relationships between them for both the left and right feet. The HS distribution indicates that both feet showed a range of HS values, and the distributions indicate variability in Heel Strike positions and intensities across different gait cycles. Similarly, the TO values for both feet display variability, reflecting differences in the Toe-Off phase of the gait cycle. The scatter plots in Figure 6 reveal the relationships between the HS and TO values for each foot, highlighting how these two parameters vary together across different gait cycles.

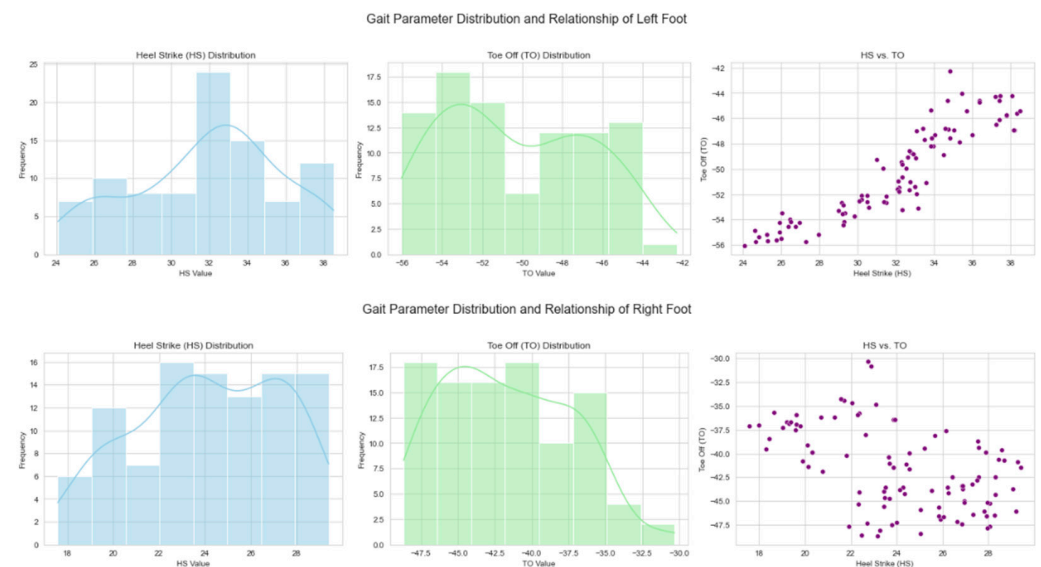


Figure 6. Gait parameter distribution. The graph (above) is for the left foot, and the graph (below) is for the right foot.

These visual comparisons allow us to observe that while there may be similarities in the distribution of gait parameters between the left and right feet, each foot exhibits unique characteristics. Figure 7 shows boxplots to compare the ranges and central tendencies of the HS and TO values. Figure 7 provides insights into the ranges, medians, and variability of these gait parameters for both feet. The boxplot of the HS values helps clarify how the Heel Strike phase might differ between the two feet in terms of intensity or position. Similarly, the boxplot of the TO values compares the distributions between the left and right feet, highlighting differences in the Toe-Off phase's timing and intensity.

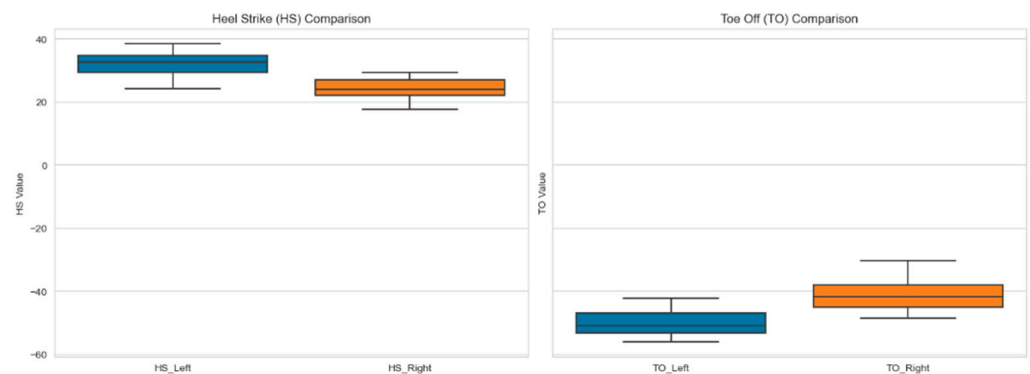


Figure 7. Comparison of gait parameters across left and right feet. The (left) graph is for HS, while the (right) graph is for TO.

4. Gait Pattern Recognition Based on Gait Feature Points

We proposed a method for identifying individuals by analyzing walking patterns using gait feature points. First, we examined whether there were significant differences in the gait parameters extracted from the subjects. Then, the gait cycles were superimposed into a single graph to identify the statistical characteristics of the gait parameters. Three feature points that can identify walking patterns were extracted. We checked whether individuals could be identified using these gait features. Finally, we analyzed the accuracy of individual identification by building several machine learning models with these feature points as a dataset.

4.1. Extraction of Gait Parameters

Gait parameters were extracted from the data obtained from the subjects, and they are summarized in Table 2. The extracted gait parameters include the stance time, swing time, gait time, and cadence. The unit of all gait parameters except cadence is seconds. In Table 2, all gait parameter values except cadence are average values. The gait cycle is a duration, as it is the time between taking a left footstep (or right footstep) and taking the next left footstep (or right footstep). The gait cycle is the sum of the stance time and swing time.

Table 2. Summary of the gait parameters extracted from the subjects.

ID	Sex	Age	Height (cm)	Stance Time/Swing Time Ratio	Gait Time (s)	Cadence
1	F	23	163	1.46	9.99	128
2	F	24	159	2.33	14.74	112
3	F	23	158	2.18	10.06	127
4	F	23	159	1.83	10.93	109
5	F	23	162	2.51	11.48	114
6	F	23	157	2.3	11.4	130
7.	F	23	156	1.97	9.84	129
8.	F	23	159	1.73	10.21	130
Avg. (female)				2.04	11.08	122.38

Table 2. Cont.

ID	Sex	Age	Height (cm)	Stance Time/Swing Time Ratio	Gait Time (s)	Cadence
9	M	25	173	2.36	10.97	106
10	M	26	173	2.43	9.59	112
11	M	23	179	2.22	8.84	115
12	M	23	190	2.29	9.6	114
13	M	25	172	2.3	11.4	130
14	M	29	182	2.28	11.46	101
Avg. (male)				2.31	10.31	113
Overall Avg.				2.16	10.75	118.36

As can be seen in Table 2, the average gait time of the male subjects was shorter than that of the female subjects. We expected that the difference in the gait cycles between the men and women would also affect the cadence values. We also predicted that there would be differences in gait time, even within the same gender or age group. There were clear differences in the gait parameters among the subjects, and based on this, we proposed a method for extracting feature points that can distinguish individual gait characteristics from the gait cycle.

4.2. Extraction of Gait Features from Superimposed Gait Cycles

The proportion of the stance phase in the gait cycle was measured to be 70%. In addition, the swing phase, which corresponded to 30% of the gait cycle, showed little variation compared to the other gait-related parameters, with the largest standard deviation being only 0.17 in each gait cycle. Therefore, we focused on the inflection point of the gait cycle curve in the section corresponding to the stance phase.

As shown in Figure 8, we can extract two points (GP1 and GP3) with the maximum and minimum values in the stance phase interval. In addition, we can identify the inflection point (GP2) in the interval (GP1, GP3). Gait feature points GP1, GP2, and GP3 can be associated with the points where Heel Strike, Mid-Stance, and Toe-Off occur in the gait segment. GP1 (Heel Strike) and GP3 (Toe-Off) are the points where the knee angle (roll value) shows its maximum and minimum values, respectively. The closed interval (GP1, GP3) corresponds to the start and end of the stance phase. Gait feature point GP2 is the point where inflection occurs and corresponds to Mid-Stance in the gait cycle. GP2 is also the point with the greatest variation between subjects. Table 3 shows the gait features extracted from the subjects.

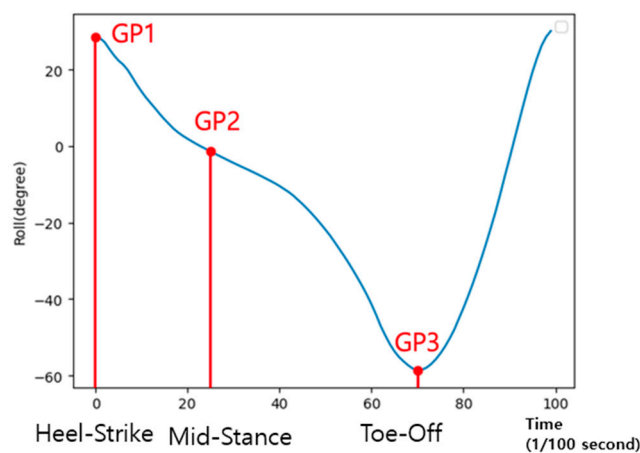


Figure 8. Extraction of feature points from the stance phase.

Table 3. The gait feature points of the subjects.

ID	Left Foot			Right Foot		
	GP1	GP2	GP3	GP1	GP2	GP3
1	23.69	−2.43	−56.27	19.17	−3.98	−48.7
2	22.14	−11.07	−48.61	19.41	−13.17	−50.88
3	18.37	−8.88	−46.8	12.84	−9.19	−40.05
4	20.13	−10.34	−56.40	16.59	−14.77	−37.35
5	24.95	−4.73	−45.01	23.25	−6.23	−49.10
6	25.42	−2.97	−51.07	25.59	−6.15	−48.93
7	28.14	−5.84	−43.90	26.60	−3.31	−61.64
8	22.41	−4.30	−54.15	18.30	−7.07	−55.38
Avg. (female)	23.16	−6.32	−50.28	20.22	−7.98	−49.0
9	27.94	−2.88	−58.91	25.50	−4.86	−56.16
10	32.51	0.72	−44.11	35.24	2.47	−51.70
11	37.60	−1.90	−44.17	30.60	−3.81	−49.51
12	26.11	−5.04	−43.08	25.50	−4.86	−56.16
13	31.85	−4.39	−50.24	25.65	−7.40	−41.92
14	31.85	−2.43	−56.27	28.17	−1.60	−43.67
Avg. (male)	31.31	−1.84	−49.46	27.08	−3.34	−49.85
Avg	26.65	−4.75	−49.93	23.74	−6.00	−49.34

4.3. Identification of Individual Gait Patterns Based on Feature Points

Figure 9 presents a 3D scatter plot showing the relationship between the values across GP1, GP2, and GP3 for each individual. In this visualization, the *x*, *y*, and *z* axes represent the GP1, GP2, and GP3 values, respectively, with the color intensity reflecting the normalized GP3 values.

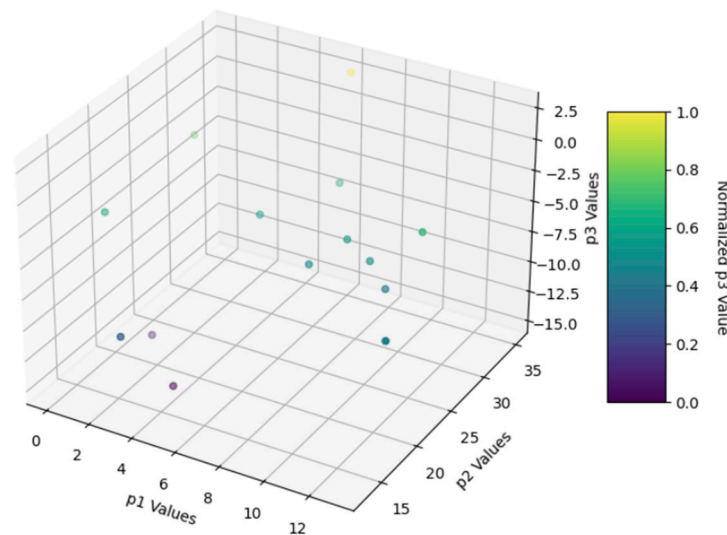


Figure 9. A 3D scatter plot showing the relationship between the values across GP1, GP2, and GP3.

This 3D perspective provides a comprehensive view of how these three dimensions correlate for each person. With only these three feature points, it is possible to distinguish each subject’s walking pattern.

4.4. MLP Model for Gait Pattern Identification

We showed that the gait features extracted through statistical modeling can be used to identify the walking patterns of the subjects. We built several machine learning models using the gait-related data as a training dataset and analyzed their classification performance.

As summarized in Table 2, the gait intervals varied from subject to subject. Since datasets for training a machine learning model must be the same size, we needed to unify the gait cycles of the different intervals. To make the different lengths of the gait cycles equal, we normalized them based on the gait cycle with the maximum period. Although the gait cycles varied between the subjects, their differences were relatively small. Thus, it was necessary to reduce the variation by minimizing the standard deviation of the gait cycles. In these experiments, we obtained an average of 10 ± 2 gait cycles. Therefore, to reduce the variation in the gait cycles (average) for each subject, we collected 100 ± 20 data by running the experiment 10 times.

The classification accuracy of each of the four machine learning models is summarized in Table 4. The classification accuracy of most models ranged from 95 to 97%. The evaluation using eXtreme gradient boosting showed a strong performance with an accuracy of 0.97, a precision of 0.97, a recall of 0.97, and an F1-Score of 0.97. This demonstrated that the gait feature-based model can be used to identify individuals.

Table 4. Classification accuracy of each model.

Model	Accuracy	Precision	Recall	F1-Score
Multi-Layer Perceptron (MLP)	0.95	0.95	0.95	0.95
Random Forest	0.95	0.95	0.95	0.95
Support Vector Machine (SVM)	0.95	0.95	0.94	0.94
eXtreme Gradient Boosting	0.97	0.97	0.97	0.97

5. Determining Whether to Use a Mobile Phone Based on Walking Pattern

To demonstrate the usability of the gait pattern identification using gait features, we applied it to a real application. We conducted an experiment to determine whether there was a significant difference between the walking patterns of those who used a mobile phone while walking and those who did not. There were a total of seven subjects (16 years old—four persons (three males and one female), 23 years old—one person (female), 26 years old—one person (male), and 29 years old—one person (male)). They walked a total of 15 m in a straight line while using their mobile phones, then walked on the same line again without using their phones. The subjects were asked to walk as normal as possible. This experiment was repeated five times.

Walking begins at the heel strike (HS) stage, the moment the heel touches the ground. At this time, the foot is placed on the ground and the leg starts to move. The toe-off (TO) stage is the moment when the sole of the foot is lifted off the ground, preparing for the next gait cycle. Among the subject's gait parameters, the HS and the TO values were visualized as a scatter plot in Figure 10. In Figure 10, the HS and the TO values when a mobile phone was not used and when used are indicated by red and blue circles, respectively. The TO average was higher in the case of not using a mobile phone than in the case of using a mobile phone. There is a clear difference in the scatter plot, enough to distinguish whether or not a mobile phone was used for most of the subjects (5 out of 7).

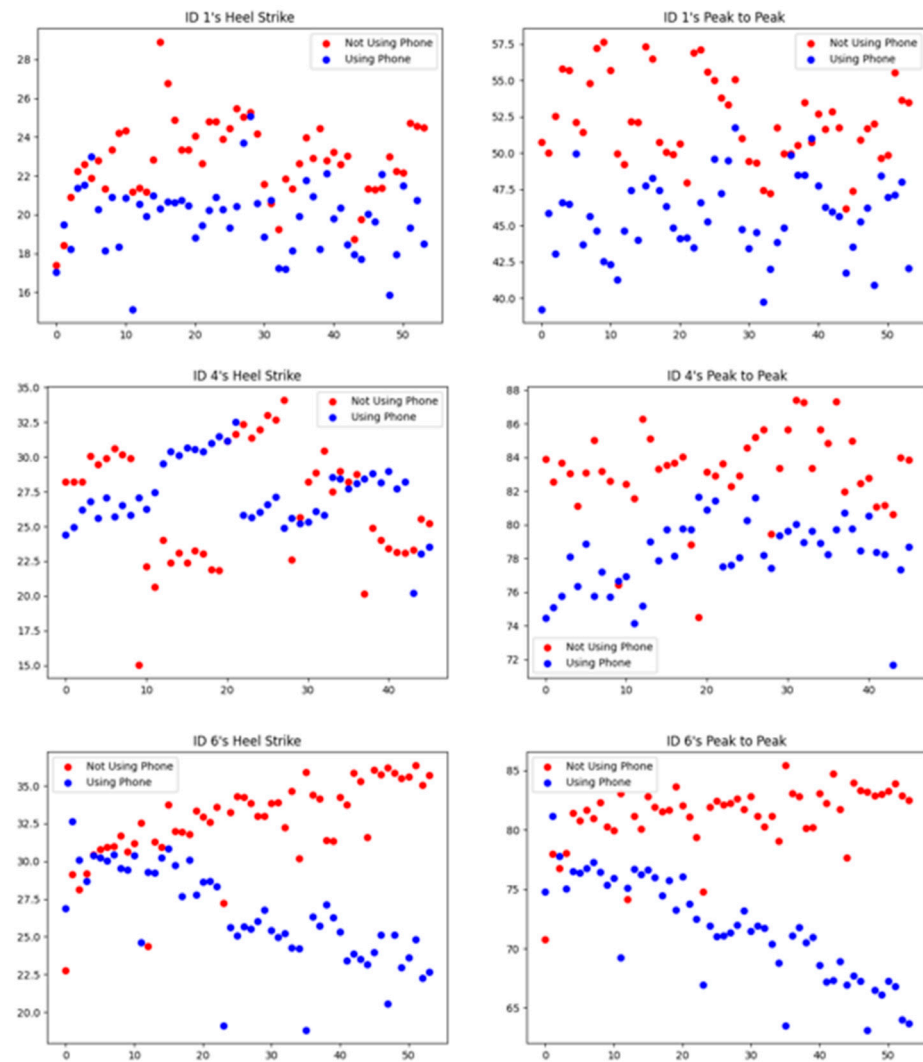


Figure 10. Heel Strike (HS) and Toe-Off (TO) distributions of subjects.

In Figure 11, shows the averages of 10 footsteps using a bar graph. The right and left bars for each subject represent the number of steps (average) when a mobile phone was or was not used, respectively. It can be seen that the number of steps taken when using a mobile phone was higher than the number of steps taken when not using a mobile phone.

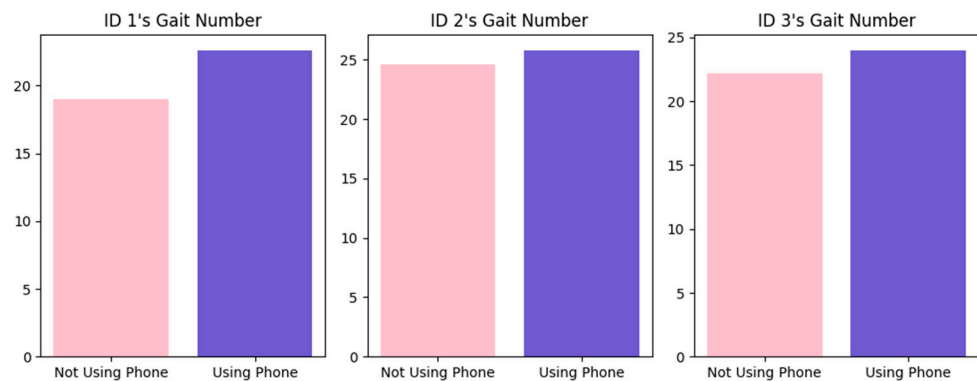


Figure 11. Gait numbers that occurred when a mobile phone was or was not used by the subjects.

Through the analysis of gait parameters, it was confirmed that mobile phone usage had a significant impact on walking patterns. The classification performance was evaluated using machine learning modeling (logistic regression and random forest) using six gait

parameters (HS, TO, PTP (peak-to-peak), gait cycle, gait number, and gait time) as a dataset. Note that HS and TO corresponded to the feature points GP1 and GP3, respectively. Even though the dataset was not large enough, the classification accuracy for both methods on the test set was 86%. The precision, recall, and F1-Score of the logistic regression model were 0.92, 0.85, and 0.88, respectively, while the precision, recall, and F1-Score of the random forest model were 1.00, 0.75, and 0.86, respectively.

6. Conclusions

In this study, we built a wearable module with an MPU-9250 IMU sensor for gait analysis. The gait cycle could be determined using roll data measured by the accelerometer built into the IMU sensor. By superimposing the gait cycles determined during the walking period, gait-related parameters could be extracted using statistical techniques. We proposed a method for identifying individuals by analyzing their walking patterns using gait feature points. We extracted two points, GP1 and GP3, with the maximum and minimum values in the stance phase interval. In addition, we could identify the point GP2, where the inflection point occurred in the interval (GP1, GP3). GP1, GP2, and GP3 could be associated with the points where Heel Strike, Mid-Stance, and Toe-Off occurred in the gait segment. Three feature points that could identify walking patterns were extracted.

To verify the feasibility of feature-based gait pattern recognition, we analyzed the accuracy of individual identification by building several machine learning models using these feature points as a dataset. The classification accuracy of most models ranged from 95 to 97%. To demonstrate the usability of the gait pattern identification using gait features, we conducted an experiment to determine whether there was a significant difference between the walking patterns of those who used a mobile phone while walking and those who did not. The classification performance was evaluated using two machine learning models and a dataset that included two gait features (HS and TO). Although the number of subjects was limited to seven, the classification accuracy of the machine learning models reached 92–100%.

Author Contributions: Conceptualization, Y.-S.H.; methodology, Y.-S.H. and W.-C.S.; software, M.-J.K. and J.-H.H.; validation, Y.-S.H., M.-J.K., and J.-H.H.; formal analysis, Y.-S.H. and W.-C.S.; investigation, M.-J.K. and J.-H.H.; resources, M.-J.K. and J.-H.H.; data curation, M.-J.K. and J.-H.H.; writing—original draft preparation, M.-J.K. and J.-H.H.; writing—review and editing, Y.-S.H.; visualization, M.-J.K. and J.-H.H.; supervision, Y.-S.H.; project administration, Y.-S.H.; funding acquisition, Y.-S.H. All authors have read and agreed to the published version of the manuscript.

Funding: This research was partially funded by Incheon National University (grant number 2023-0144).

Institutional Review Board Statement: This study was conducted in accordance with the Declaration of Helsinki and was approved by the Institutional Review Board of Incheon National University (7007971-202303-004, 18 May 2023).

Informed Consent Statement: Not applicable.

Data Availability Statement: All data used in this paper were dependent on the sensors used and the measurement environments. The measurement values of each sensor used in our experiments will be provided upon request by e-mail.

Conflicts of Interest: The authors declare no conflicts of interest.

References

1. Montero-Odasso, M.; Verghese, J.; Beauchet, O.; Hausdorff, J.M. Gait and Cognition: A complementary approach to understanding brain function and the risk of falling. *J. Am. Geriatr. Soc.* **2012**, *60*, 2127–2136. [[CrossRef](#)] [[PubMed](#)]
2. Beauchet, O.; Allali, G.; Berrut, G.; Hommet, C.; Dubost, V.; Assal, F. Gait analysis in demented subjects: Interests and perspectives. *Neuropsychiatr. Dis. Treat.* **2008**, *4*, 155–160. [[CrossRef](#)] [[PubMed](#)] [[PubMed Central](#)]
3. Allali, G.; Kressig, R.W.; Assal, F.; Herrmann, F.R.; Dubost, V.; Beauchet, O. Changes in gait while backward counting in demented older adults with frontal lobe dysfunction. *Gait Posture* **2007**, *26*, 572–576. [[CrossRef](#)] [[PubMed](#)]
4. Lee, N.G.; Kang, T.W.; Park, H.J. Relationship Between Balance, Gait, and Activities of Daily Living in Older Adults with Dementia. *Geriatr. Orthop. Surg. Rehabil.* **2020**, *11*, 2151459320929578. [[CrossRef](#)] [[PubMed](#)]

5. Vu, H.T.T.; Dong, D.; Cao, H.L.; Verstraten, T.; Lefeber, D.; Vanderborght, B.; Geeroms, J. A Review of Gait Phase Detection Algorithms for Lower Limb Prostheses. *Sensors* **2020**, *20*, 3972. [[CrossRef](#)] [[PubMed](#)] [[PubMed Central](#)]
6. Kanwar, A.; Upadhyay, P. An appearance-based approach for gait identification using infrared imaging. In Proceedings of the 2014 International Conference on Issues and Challenges in Intelligent Computing Techniques (ICICT), Ghaziabad, India, 7–8 February 2014; pp. 719–724. [[CrossRef](#)]
7. Prakash, C.; Gupta, K.; Mittal, A.; Kumar, R.; Laxmi, V. Passive Marker Based Optical System for Gait Kinematics for Lower Extremity. *Procedia Comput. Sci.* **2015**, *45*, 176–185. [[CrossRef](#)]
8. Kwolek, B.; Michalczuk, A.; Krzeszowski, T.; Switonski, A.; Josinski, H.; Wojciechowski, K. Calibrated and synchronized multi-view video and motion capture dataset for evaluation of gait recognition. *Multimed. Tools Appl.* **2019**, *78*, 32437–32465. [[CrossRef](#)]
9. Carse, B.; Meadows, B.; Bowers, R.; Rowe, P. Affordable clinical gait analysis: An assessment of the marker tracking accuracy of a new low-cost optical 3D motion analysis system. *Physiotherapy* **2013**, *99*, 347–351. [[CrossRef](#)] [[PubMed](#)]
10. Aqueveque, P.; Germany, E.; Osorio, R.; Pastene, F. Gait Segmentation Method Using a Plantar Pressure Measurement System with Custom-Made Capacitive Sensors. *Sensors* **2020**, *20*, 656. [[CrossRef](#)] [[PubMed](#)] [[PubMed Central](#)]
11. Kim, H.; Kang, Y.; Valencia, D.R.; Kim, D. An Integrated System for Gait Analysis Using FSRs and an IMU. In Proceedings of the 2018 Second IEEE International Conference on Robotic Computing (IRC), Laguna Hills, CA, USA, 31 January–2 February 2018; pp. 347–351. [[CrossRef](#)]
12. Lin, C.-L.; Fan, K.-C.; Lai, C.-R.; Cheng, H.-Y.; Chen, T.-P.; Hung, C.-M. Applying a Deep Learning Neural Network to Gait-Based Pedestrian Automatic Detection and Recognition. *Appl. Sci.* **2022**, *12*, 4326. [[CrossRef](#)]
13. Lee, S.-B.; Lee, S.-J.; Park, E.; Lee, J.; Kim, I. Gait-based continuous authentication using a novel sensor compensation algorithm and geometric features extracted from wearable sensors. *IEEE Access* **2022**, *10*, 120122–120135. [[CrossRef](#)]
14. Seel, T.; Raisch, J.; Schauer, T. IMU-Based Joint Angle Measurement for Gait Analysis. *Sensors* **2014**, *14*, 6891–6909. [[CrossRef](#)] [[PubMed](#)]
15. Moon, K.S.; Lee, S.Q.; Ozturk, Y.; Gaidhani, A.; Cox, J.A. Identification of Gait Motion Patterns Using Wearable Inertial Sensor Network. *Sensors* **2019**, *19*, 5024. [[CrossRef](#)] [[PubMed](#)]
16. Lee, T.; Kim, I.; Lee, S.-H. Estimation of the Continuous Walking Angle of Knee and Ankle (Talocrural Joint, Subtalar Joint) of a Lower-Limb Exoskeleton Robot Using a Neural Network. *Sensors* **2021**, *21*, 2807. [[CrossRef](#)] [[PubMed](#)]
17. Shin, D.; Lee, S.; Hwang, S. Locomotion Mode Recognition Algorithm Based on Gaussian Mixture Model Using IMU Sensors. *Sensors* **2021**, *21*, 2785. [[CrossRef](#)]
18. Gujarathi, T.; Bhole, K. Gait Analysis Using IMU Sensor. In Proceedings of the 2019 10th International Conference on Computing, Communication and Networking Technologies (ICCCNT), Kanpur, India, 6–8 July 2019; pp. 1–5. [[CrossRef](#)]
19. Park, S.; Yoon, S. Validity Evaluation of an Inertial Measurement Unit (IMU) in Gait Analysis Using Statistical Parametric Mapping (SPM). *Sensors* **2021**, *21*, 3667. [[CrossRef](#)] [[PubMed](#)] [[PubMed Central](#)]
20. Hacker, S.; Kalkbrenner, C.; Algorri, M.-E.; Blechschmidt, R. Gait Analysis with IMU. Gaining New Orientation Information of the Lower Leg. In Proceedings of the International Joint Conference on Biomedical Engineering Systems and Technologies (BIOSTEC 2014), Angers, Loire Valley, France, 3–6 March 2014. [[CrossRef](#)]
21. Prasanth, H.; Caban, M.; Keller, U.; Courtine, G.; Ijspeert, A.; Vallery, H.; Von Zitzewitz, J. Wearable Sensor-Based Real-Time Gait Detection: A Systematic Review. *Sensors* **2021**, *21*, 2727. [[CrossRef](#)] [[PubMed](#)]
22. Han, Y.C.; Wong, K.I.; Murray, I. Gait Phase Detection for Normal and Abnormal Gaits Using IMU. *IEEE Sens. J.* **2019**, *19*, 3439–3448. [[CrossRef](#)]
23. Pirker, W.; Katzenschlager, R. Gait disorders in adults and the elderly: A clinical guide. *Wien. Klin. Wochenschr.* **2016**, *129*, 81–95. [[CrossRef](#)] [[PubMed](#)]

Disclaimer/Publisher’s Note: The statements, opinions and data contained in all publications are solely those of the individual author(s) and contributor(s) and not of MDPI and/or the editor(s). MDPI and/or the editor(s) disclaim responsibility for any injury to people or property resulting from any ideas, methods, instructions or products referred to in the content.